

Micelle Formation in Mixtures of Styrene–Isoprene Diblock Copolymer and Poly(vinyl methyl ether)

Jong-Hyun Ahn, Byeong-Hyeok Sohn, and Wang-Cheol Zin*

Department of Materials Science & Engineering and Polymer Research Institute,
Pohang University of Science and Technology, Pohang, 790-784, Korea

Si-Tae Noh

Department of Chemical Engineering, Hanyang University, Ansan, 425-791, Korea

Received September 25, 2000

ABSTRACT: The characteristics of micelle formed in blends of styrene–isoprene diblock copolymer (SI) and poly(vinyl methyl ether) (PVME) were investigated by using small-angle X-ray scattering (SAXS), transmission electron microscopy (TEM), and light scattering techniques. The results of SAXS and TEM experiments indicate that the blends form spherical micelles with isoprene-rich cores and styrene–corona mixed with PVME in a matrix of PVME. As temperature increased, the blends underwent macrophase separation into a PVME-rich phase and a SI-rich phase which was also microphase-separated to ordered microdomains. Upon further heating, the ordered structure of the SI-rich region transforms to a disordered phase in a manner resembling the order–disorder transition in pure block copolymer melts.

I. Introduction

In a block copolymer consisting of chemically different, immiscible polymer chains, the blocks segregate out into their own microdomains, forming a variety of ordered macrolattice such as the lamellar, gyroid, hexagonally ordered cylindrical, and spherical phases.^{1,2} When a block copolymer is mixed with a homopolymer, the blend exhibits complex phase behaviors.^{3–7} Homogeneous mixtures, macrophase separation, and the formation of different mesophases can occur, depending on the temperature and composition. In addition, when a small amount of block copolymer is added to homopolymer, the copolymer segregates to form micelles dispersed in the homopolymer matrix.^{8–15}

A number of studies on binary blends of a diblock copolymer (A–B) and a homopolymer (H) has been reported in recent literature. However, these investigations have focused mainly on systems where H is chemically identical with the one block of block copolymer.^{3–15} Only a few studies have dealt with the phase relations and miscibility in blends of an A–B diblock with a third homopolymer H that is miscible with one block but immiscible with the other block.^{16–22} It is well-known that blends of polystyrene (PS) with PVME exhibit a lower critical solution temperature (LCST) which is one of the characteristic phenomena in a miscible blend.^{23–26} In the case where PVME is mixed with a styrene–isoprene diblock copolymer (SI) having an ordered microdomain structure, the PVME might be preferably dissolved into the styrene microdomains of the copolymer due to the specific interaction. In the previous work, we presented the phase diagrams of binary blends of SI and PVME exhibiting a fascinating complexity.^{20,21} However, the region of the phase diagram involving the small amounts of SI mixed with much larger amounts of PVME was not investigated in detail in the previous study.²¹

In this paper, we focus our attention on the micelle formation and phase behavior of the mixture where the fraction of SI is much less than that of PVME. The micelle cores consist of aggregated isoprene blocks that are surrounded by a corona region containing PS blocks swollen with PVME. The PVME matrix will contain a small amount of dissolved copolymer. We also examine the effect of specific segmental interaction between SI and PVME on micelle formation.

II. Experimental Section

Materials. The characteristics of the polymers used are listed in Table 1. Styrene–isoprene diblock copolymer (SI72) and homopolystyrenes (HPS75 and HPS48) were synthesized by living anionic polymerization using high-vacuum techniques. Neat SI72 has microdomain morphology of polyisoprene cylinders in a polystyrene matrix. PVME was commercially available materials (Aldrich Co.). It was dissolved by toluene, purified by activated carbon powder, and precipitated twice by a large excess of *n*-hexane. Blends of SI72/PVME and SI72/HPS75 with various fractions were prepared by casting from toluene solution in the presence of an antioxidant (Irganox 1010, Ciba-Geigy Group) and then slowly evaporating the solvent for 5 days. The samples were then dried under vacuum at room temperature over a period of 1 week. In the case of SI72/HPS75 blends, the dried samples were further annealed under vacuum at 120 °C for 1 day to have equilibrium morphologies. Blends of HPS48/PVME were also prepared in the same manner only for the purpose of cloud point measurements.

Small-Angle X-ray Scattering. Small-angle X-ray scattering (SAXS) measurements were performed with point focusing (0.2 × 0.2 mm) at 1B2 beamline (1.377 Å in wavelength) and 3C2 beamline (1.540 Å in wavelength) using synchrotron X-ray radiation sources at Pohang Accelerator Laboratory, Korea. A one-dimensional position-sensitive detector (model 1412XR, EG&G Princeton Applied Research) was employed with an interface system (model 1463, EG&G). The distance between sample and detector was 1.2 m. The samples were held in an aluminum holder which was sealed with a window of 8 μm Kapton film, and then, the aluminum holder was inserted into the brass frame fastened by screws to prevent the sample from leaking out of the aluminum holder upon subsequent heating and cooling. Such samples had the

* To whom correspondence should be addressed. e-mail wczin@postech.ac.kr; Tel +82-54-279-2136; Fax +82-54-279-2399.

Table 1. Characteristics of the Polymers Used

sample code	M_w	M_w/M_n^b	styrene content ^c (wt %)
SI72	35 000 ^a	1.02	72
PVME	81 000 ^a	1.69	
HPS75	75 000 ^b	1.05	100
HPS48	47 500 ^b	1.06	100

^a By low-angle laser light scattering (LALLS). ^b By GPC calibrated with PS standard. ^c By ¹H NMR.

thickness of about 1 mm. Each sample was heated to 290 °C at a rate of 2 °C/min while the data of intensity were collected through the detector and computer interface at every 2.5 min for 1 min. The measured SAXS intensity was corrected for the decrease of the ring current, background scattering, and absorption by sample. Additional X-ray scattering measurements were conducted with an apparatus consisting of a 18 kW rotating anode X-ray generator (Rigaku Co.) operated at 50 kV × 20 mA, mirror optics with point focusing, and a one-dimensional position-sensitive detector (M. Braun Co.). The Cu K α radiation (=1.542 Å) from a 0.1 × 1 mm microfocus cathode was used. The data are presented as a function of $q = 4\pi(\sin \theta)/\lambda$, where 2θ is the scattering angle and λ is the X-ray wavelength.

We may say that the possible degradation of sample during the measurement did not affect the phase behavior since SAXS patterns of block copolymer did not reveal any noticeable differences between first and second heating.

The following specific volume values were used to calculate the electron density at various temperatures.^{10,26}

$$V_{\text{PS}}(\text{PS}) = 0.9369 + 2.006 \times 10^{-4}T + 2.470 \times 10^{-7}T^2 \quad (\text{below } T_g)$$

$$V_{\text{PI}}(\text{PI}) = 1.0771 + 7.22 \times 10^{-4}T + 2.46 \times 10^{-7}T^2$$

$$V_{\text{PVME}}(\text{PVME}) = 1/(1.0725 - 7.259 \times 10^{-4}T + 1.160 \times 10^{-7}T^2)$$

where T denotes the temperature in degrees centigrade.

Transmission Electron Microscopy. The RMC (MT-7000) cryoultramicrotome system was used to obtain ultrathin section (~90 nm) for TEM. Microtoming was conducted at -120 °C below the glass transition temperatures of PI and PVME using a diamond knife. Sections were picked up on 300-mesh uncoated copper grids and then stained by the vapor of 2% aqueous OsO₄ solution. TEM was performed on a JEOL 1200EX electron microscope operated at 120 kV.

Cloud Point Measurements. The cloud temperature was determined by monitoring the intensity of scattered light at 40° through the blend film located on a hot stage. A He-Ne laser (4 mW) was used as a light source. The scattered intensity was measured at a constant heating/cooling rate of 2 °C/min by a photodiode detector (Newport Corp. 835 optical power meter).

Data Analysis of SAXS Measurements. The micelle core with the dense isoprene block chains is surrounded by a corona of styrene block chains swollen with PVME. Since the electron density of PVME ($\rho = 349 \text{ e/nm}^3$ at room temperature) is almost equal to PS ($\rho = 340 \text{ e/nm}^3$), it can be considered that PVME matrix has the same electron density as the corona region.

The scattered intensity $I(q)$ from a system of particle can be written as a product of the single particle form factor, $F(q)$, and a structure factor, $S(q)$, which describes the interparticle interference:

$$I(q) = (\Delta\rho)^2 N |F(q)|^2 S(q) \quad (1)$$

where $\Delta\rho$ is the electron density difference between the micelle core and their surroundings and N is the number density of micelles.

For a homogeneous sphere of radius R , the form factor is defined by

$$F(q) = \frac{4\pi}{q^3} [\sin(qR) - qR \cos(qR)] \quad (2)$$

Using the classical Ornstein–Zernike approximation for the spatial correlation fluctuations and the Percus–Yevick (PY) approximation for hard-sphere fluids, the structure factor is given by^{27,28}

$$S(q) = \frac{1}{1 + 24\eta G(2qR_{\text{HS}}, \eta)/(2qR_{\text{HS}})} \quad (3)$$

where G is a trigonometric function of R_{HS} and η is the hard-sphere volume fraction ($\eta = 4\pi NR_{\text{HS}}^3/3$).

For these micellar systems, there will inevitably be some distribution in the size of the micelle core and the corona region. To observe the effects of polydispersity of particles, eq 1 is rewritten by^{10,29}

$$I(q) = (\Delta\rho)^2 N |F(q)|^2 S'(q) \quad (4)$$

where $S'(q)$ acts as an apparent structure factor. By assuming that particle size and position are uncorrelated, it is defined by

$$S'(q) = 1 + \beta(q)[S(q) - 1] \quad (5)$$

where

$$\beta(q) = \langle |F(q)|^2 \rangle / \langle |F(q)| \rangle^2 \quad (6)$$

To evaluate the average of the form factor $F(q)$, we assume the micelle core radii to be distributed according to the Flory–Schultz distribution

$$W(R) = (1/Z)b^{Z+1}R^Z \exp(-bR) \quad (7)$$

where the parameter Z characterizes the width of the distribution ($Z = \infty$ corresponding to a δ function) and the parameter b is related to the number-average radius $\langle R \rangle$ by $b = (Z + 1)/\langle R \rangle$. The root-mean-square deviation from the mean is given by $\sigma_R = (\langle R^2 \rangle - \langle R \rangle^2)^{1/2} = \langle R \rangle / (Z + 1)^{1/2}$.

The scattering function can thus be expressed in an analytical form with only four parameters: the parameters Z , $N(\Delta\rho)^2$, and two radii characterizing the micelles, the micelle core radius, $\langle R_c \rangle$, and effective hard-sphere radius, $\langle R_{\text{HS}} \rangle$. The fitting to the experimental scattering patterns has been obtained from nonlinear least-squares fitting procedure.

III. Results and Discussion

Micelle Structure. At low block copolymer concentration, a homogeneous phase may occur in which the SI block copolymer is molecularly dispersed in the PVME matrix. As the copolymer concentration is increased beyond the critical micelle concentration, the isoprene blocks begin to aggregate, and micelles are expected to be formed in which the core contains the isoprene blocks and the corona region contains both the styrene blocks and PVME homopolymer as seen in Figure 1. These micelles are randomly dispersed, without long-range ordering, in the PVME matrix, which contains a small amount of dissolved copolymer.

Figure 2 shows the TEM images observed for blends containing 5 and 10 wt % copolymer. The dark circular regions are the spherical micelle cores consisted of the isoprene blocks. The images show that the spherical micelles are randomly dispersed in the homopolymer matrix and the number density of micelles increases as the copolymer concentration is increased.

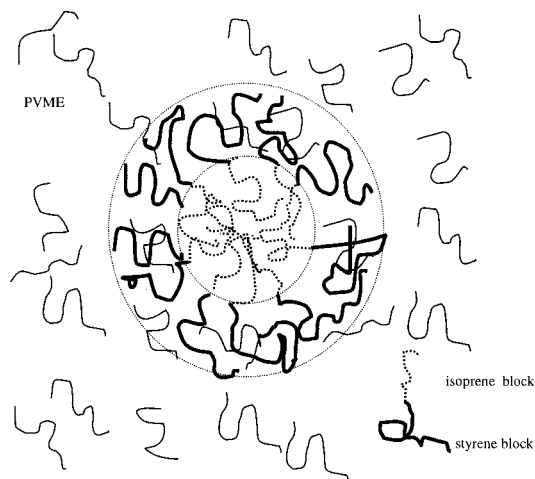


Figure 1. Schematic showing the structure of spherical micelles in blends of styrene–isoprene diblock copolymer and PVME.

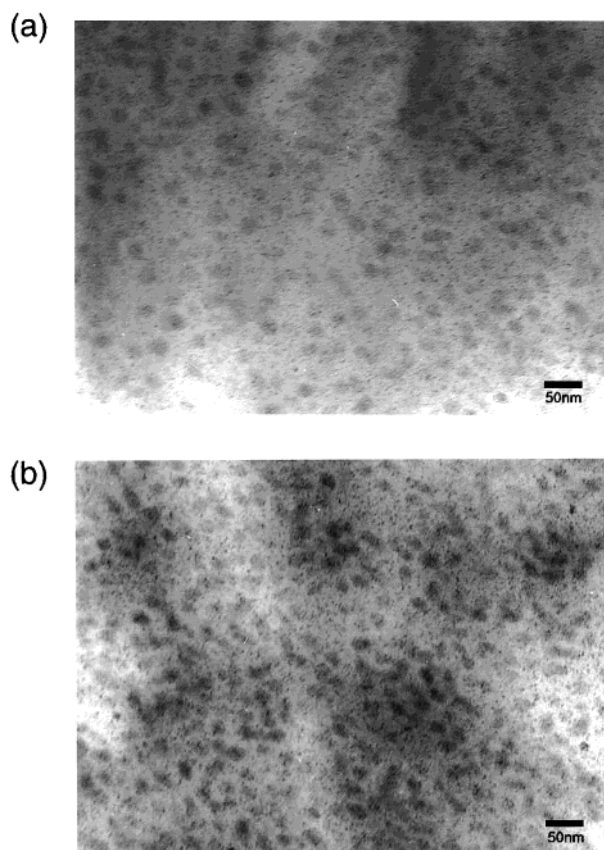


Figure 2. TEM images of blends containing (a) 5 wt % and (b) 10 wt % copolymer.

Figure 3 shows SAXS patterns for SI72/PVME blends at 35 °C. At low concentration of the copolymer (1 and 3 wt %), the SAXS patterns exhibit a characteristic of the micellar scattering at very low scattering vector, q . Upon further increase of SI72 fraction, the intensity curves show a maximum by the increased contribution of the interparticle interference. These profiles were fitted by the theoretical curves of the polydisperse hard-sphere model described in previous section. The fitting curves are shown by dotted lines in Figure 3. For example, the best values of parameters obtained for the blend containing 10 wt % copolymer are $Z = 43.27$, $\langle R_{HS} \rangle = 18.75$ nm, $\langle R_c \rangle = 8.80$ nm, and $N(\Delta\rho)^2 = 1.698 \times 10^{-2} \text{ e}^2 \text{ nm}^{-3}$.

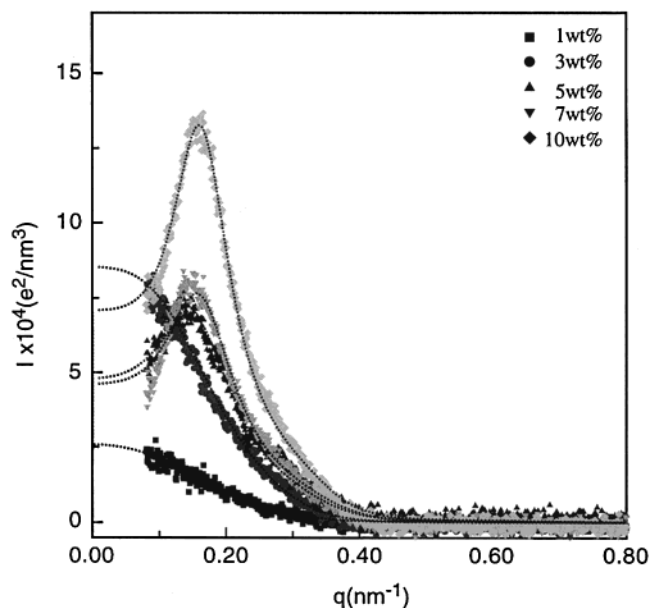


Figure 3. Scattered X-ray intensity obtained from various block copolymer concentrations. The dotted lines show the best fit to the SAXS data calculated by the polydisperse PY hard-sphere model.

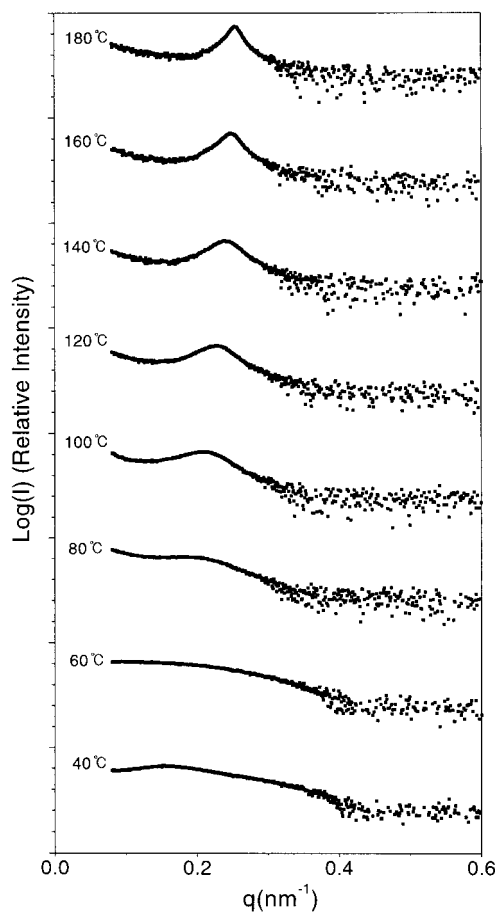


Figure 4. Temperature dependence of SAXS profiles for the blends containing 10 wt % block copolymer.

The SAXS profiles for the blend containing 10 wt % copolymer in the temperature range from 40 to 180 °C are shown in Figure 4. The scattered intensity from isolated micelle gradually disappears in magnitude as the temperature is raised. Above 60 °C, however, the peak begins to appear at the low- q position, signaling

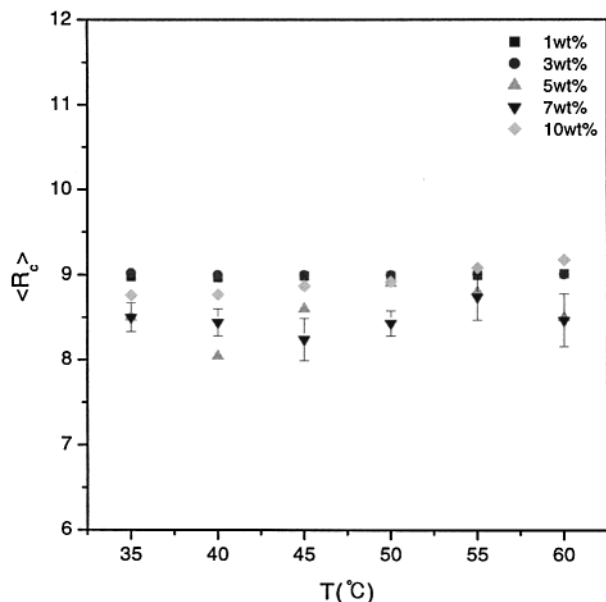


Figure 5. Radius of micelle core obtained from the PY hard-sphere model. The estimated errors are indicated for the 7 wt % blend. The errors for other blends are comparable.

the onset of demixing between SI72 and PVME. The phase behavior related to the macrophase separation between SI72 and PVME will be in detail discussed in following section.

Figure 5 shows the values of the number-average radius $\langle R_c \rangle$ of the micelle core with temperature. The core radius remains a fairly constant value up to the macrophase separation temperature, 60 °C, and is relatively independent of the concentration. Although the value of $\langle R_c \rangle$ is lower for the blends containing 5 and 7 wt % copolymer than other concentrations, it is within the experimental error.

The critical micelle concentration (cmc) can be determined by means of the invariant, Q , defined by

$$Q = \frac{1}{2\pi^2} \int q^2 I(q) dq \quad (8)$$

When the value of Q is plotted against the concentration, a fairly good straight line is obtained as seen in Figure 6. On extrapolating Q to zero, the cmc can be accurately obtained; the value of 0.15 wt % is obtained.

Figure 7 shows the number density, N , of micelles as a function of temperature for the blends of different concentrations. It is found that the values of N tend to increase as the concentration is raised and is also insensitive to the change in temperature.

The number density, N , of micelles and the volume fraction, ξ , of isoprene units within the micelle core are related to each other through the following equation:

$$\Phi = NV_{\text{core}}\xi + \Phi_c \left(1 - NV_{\text{core}} \left(\frac{R_{\text{HS}}}{R_c} \right)^3 \right) \quad (9)$$

where V_{core} denotes the micelle core volume and Φ and Φ_c denote the concentration (volume fraction) of isoprene units in the mixture and the overall isoprene concentration at cmc, respectively. In the temperature range 35–60 °C, the ξ values remain close to unity for all concentrations, indicating that the solubilization of PVME in the micelle core is very limited.

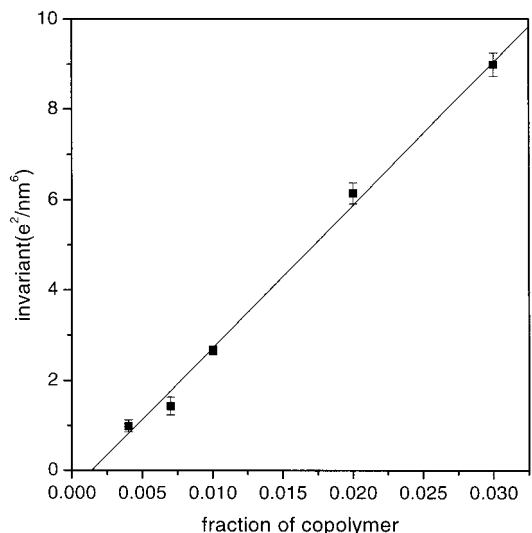


Figure 6. Determination of critical micelle concentration by the calculated invariant for SI72/PVME blend.

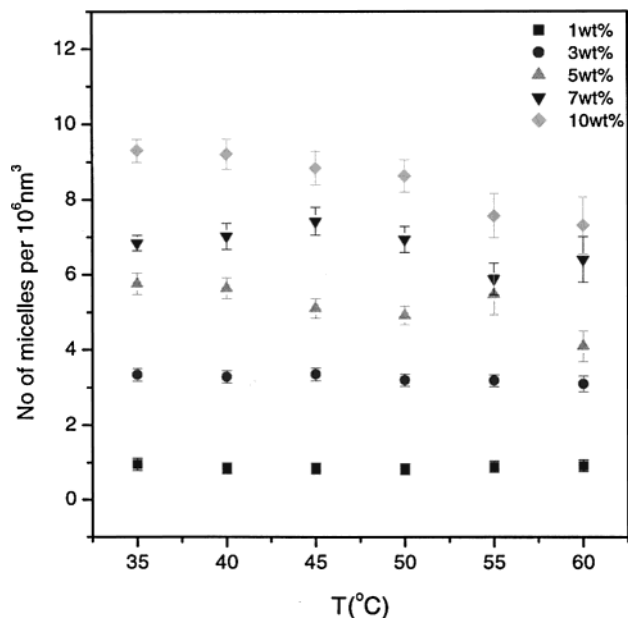


Figure 7. Number of micelles presenting in 10^6 nm^3 of the blends.

From the micelle core radius obtained in Figure 5, and with assumption that the micelle core consists of only the isoprene blocks, the number of block copolymer molecules per micelle, p , can be estimated by the following equation

$$p = \frac{4}{3} \pi R^3 / \nu_{\text{PI}} \quad (10)$$

where ν_{PI} is the molecular volume of an isoprene block given by

$$\nu_{\text{PI}} (\text{nm}^3) = \frac{M_{\text{PI}}}{\rho_{\text{PI}} (\text{g}/\text{cm}^3) \cdot 0.602 \times 10^3} \quad (11)$$

Values for p are fairly constant from 140 to 180 with temperature and concentrations, reflecting the general trend in core radius.

Kim et al. reported that the degree of exothermic interaction between the matrix polymer and one block

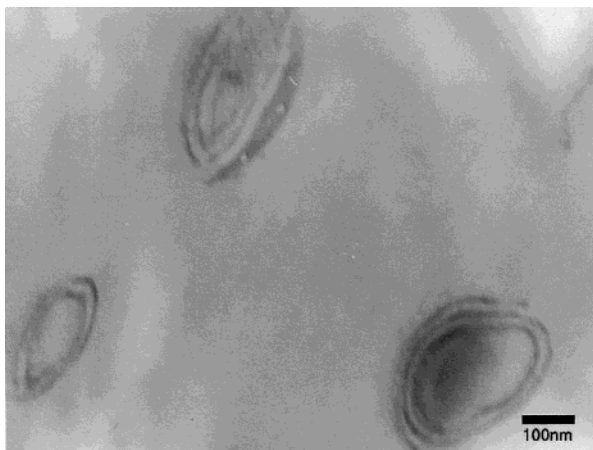


Figure 8. TEM image from the blend of SI72/HPS75 (10 wt %:90 wt %).

of the block copolymer influences the morphology and droplet sizes of the blend.³⁰ The favorable interaction energy density between styrene block chains and PVME matrix can also affect the micelle structure of SI72 and PVME blends. To see the effect of interaction energy density on micelle structure, we prepared the mixture of SI72 in the matrix of PS having the same molecular weight as PVME.

Figure 8 shows a TEM micrograph of the SI72/HPS75 (10 wt %:90 wt %) mixture. The micrograph clearly indicates the existence of macroscopic domains rich in SI72 dispersed in the matrix of HPS75 without forming spherical microdomains. It is notable that SI72/HPS75 mixture does not form the spherical micelle where HPS75 has the same molecular weight as PVME. This behavior is a consequence of the effect of homopolystyrene (HPS) molecular weight on the miscibility between styrene block and HPS. As the ratio of HPS to styrene block molecular weight, r , increases, the loss of conformational entropy in both HPS and styrene block chains increases. This increased loss of entropy reduces the miscibility between styrene block and HPS, and HPS chains may be segregated out from SI, forming a macrophase-separated morphology. For SI diblock copolymer and HPS mixture, Koizumi et al. have reported that, in the regime of $r < 1$, HPS tends to be solubilized into the microdomain of styrene block and to swell the styrene chains, but at $r > 1$, macrophase separation occurs.^{31,32} According to their results, it is expected that SI72/HPS75 blend with $r = 3$ undergoes macrophase separation.

Compared to the case of SI72/HPS75 mixture, in the case of SI72/PVME blend with attractive interactions between styrene block and PVME, PVME can be solubilized into styrene block by the negative mixing enthalpy and swell the styrene chains, causing a change in microdomain morphology. Hence, spherical micelles are formed at the limit of large volume fraction of PVME. Thus, one can see that the attractive interactions between styrene block of copolymer and PVME induce significantly the enthalpic driving force responsible for the SI72 block copolymer micellization.

Phase Behavior. The turbidity measurements were performed for the SI72/PVME blend, and the results are shown in Figure 9. The LCST behavior is clearly seen in this figure. The SI72/PVME blend exhibits lower cloud point temperature (T_{cl}) than the HPS48/PVME blend even though the molecular weight of the styrene

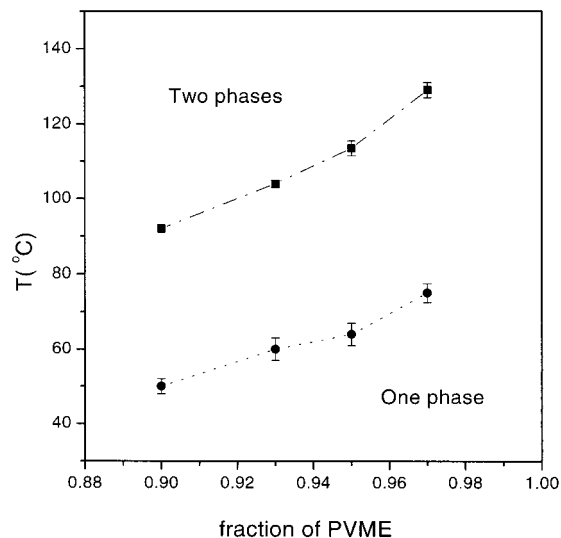


Figure 9. Cloud points curves for (●) SI72/PVME and (■) HPS48/PVME blends.

blocks of SI72 is lower than that of HPS48. It can be explained by the effect of chain confinement.^{22,24} In the case of SI block copolymer, one end of the styrene block chain is confined within the surface of isoprene micelle core, and this confinement of the chains gives rise to the mixing entropy loss, which is unfavorable to the mixing of PVME and the styrene block. Thus, by the chain confinement, the SI72/PVME blend has lower segregation temperature than PS/PVME blend.

It is worthwhile to note the difference of the phases formed above and below T_{cl} . In the one-phase region below T_{cl} , the blends form the single-phase state where PVME is mixed with styrene blocks forming corona of micelle. On the other hand, the two phases, rich in SI72 and rich in PVME, are formed above T_{cl} , where the styrene block–corona phase-separates from PVME. It is noted that the formation of interdomain peak, as seen in SAXS profiles of Figure 4, and the observed cloud points arise at almost the same temperature, presumably by the segregation of the styrene blocks from PVME.

The SAXS profiles for the blend containing 5 wt % block copolymer are given in Figure 10a, from which we observe a discontinuous change in SAXS profile at temperature between 270 and 280 °C, reflecting an order–disorder transition (ODT). To facilitate comparison with results from pure block copolymer, the square of half-width (σ_q^2) of the first-order scattered peak is plotted against $1/T$ in Figure 10b. Although the discontinuity for 5 wt % blend appears less pronounced than for the pure block copolymer, the ODT temperature of 5 wt % blend is in good agreement with that of pure block copolymer ($T_{ODT} = 275 \pm 5$ °C). In the blends containing 3, 7, and 10 wt % copolymer the observed ODT temperatures are almost the same within an experimental error.

It is interesting to note that the ODT temperatures of the blends are close to that of pure SI72. Figure 11 exhibits the change in interdomain distance determined from the first scattering maxima of SAXS profiles for pure SI72 and the blends containing 3, 5, 7, and 10 wt % copolymer. With increasing temperature the blends are separated into two phases of the SI72-rich phase and the PVME-rich phase due to the decrease in the favorable specific interaction between the styrene block

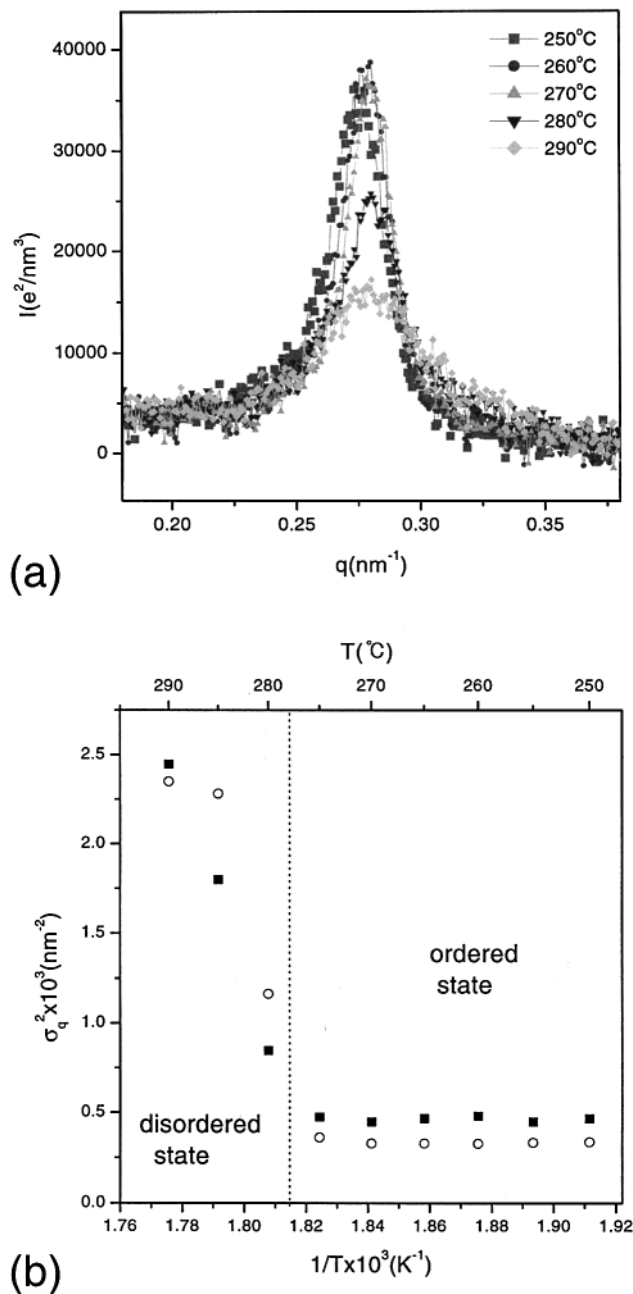


Figure 10. (a) Temperature dependence of the SAXS profile for the blend containing 5 wt % block copolymer. (b) Plot of the square of half-width of the first-order scattering maximum (σ_q^2) vs the reciprocal of absolute temperature ($1/T$) for (■) 5 wt % and (○) pure SI72. The dash line indicates the ODT temperature.

and PVME. In the SI72-rich phase, the local concentration of PVME decreases by the enhancement of demixing between SI72 and PVME, so that the interdomain distance of the blends is reduced on heating. As shown in figure, the interdomain distances of pure SI72 and blends begin to overlap above 230 °C. This implies the very limited miscibility or the complete separation between SI72 and PVME above 230 °C. Therefore, we can assume that the microdomain structure of the blends above 230 °C may be similar to that of pure SI72, even though any highly ordered scattering peak enough to prove morphology cannot be observed in scattering pattern of the blends above 230 °C.

In Figure 12, the phase diagram for SI72/PVME blends is constructed with transition temperatures

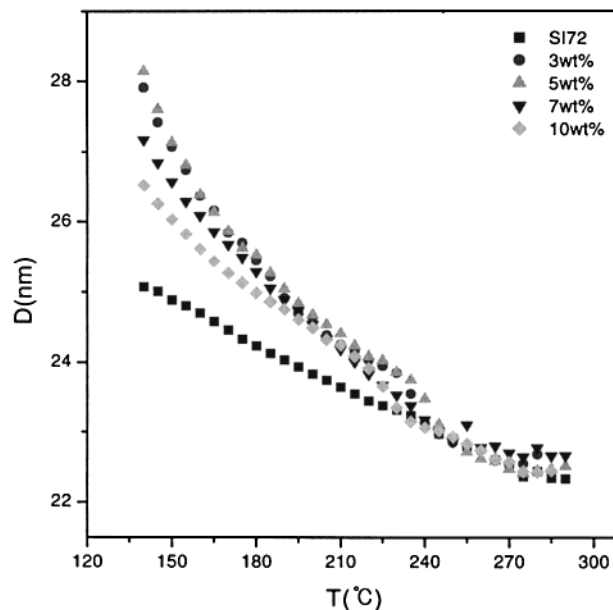


Figure 11. Variation of interdomain distance as a function of temperature for pure SI72 and the blends containing 3, 5, 7, and 10 wt % block copolymer.

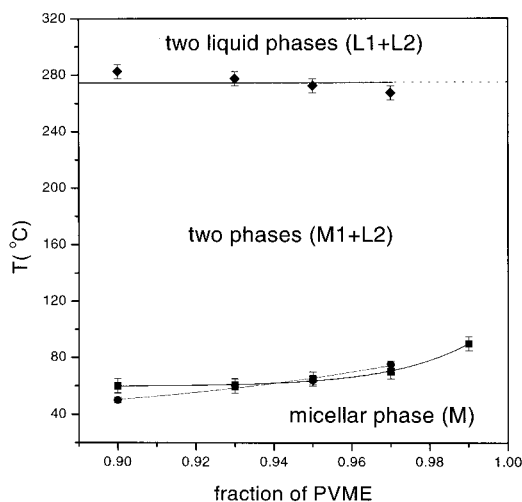


Figure 12. Phase diagram of SI72/PVME blend obtained from experimental results. As for the macrophase separation temperatures, the squares denote the results of the SAXS experiments and the circles those of the light scattering experiments. The diamonds denote the ODT temperature evaluated from the SAXS.

identified from SAXS and light scattering. There is a good agreement between the cloud points and the demixing temperatures determined by SAXS. At low temperature, the mixture forms a single micellar phase (M). Above LCST, M is separated into two phases of a mesophase (M1) and a liquid phase (L2) having different PVME fractions, where M1 phase may have the periodic microdomain structure. On further heating, M1 undergoes the transition from an ordered to a disordered phase (L1). For the blends of 3, 5, 7, and 10 wt %, the observed ODT temperatures are indicated in this figure with diamonds. (In the case of 1 wt % blend, the ODT cannot be determined because of a very low scattered peak.)

IV. Conclusions

SAXS, TEM, and light scattering have been used to investigate the micellar structure and the phase behav-

ior of the styrene–isoprene diblock copolymer and PVME blend. At low temperature, the copolymers form the spherical micelles in the matrix of PVME. On the other hand, in the matrix of polystyrene having the same molecular weight as PVME, macrophase separation was observed to occur. These led us to conclude that the micelle formation of SI72/PVME blend is strongly dependent on attractive interactions between styrene block and PVME. The core radius and hard-sphere interaction radius of the spherical micelles were obtained by fitting appropriate models to the SAXS patterns. The micelle core radii were about 9 nm, independent of block copolymer concentration. The predicted core radius was in good agreement with TEM result. In addition, it was found that the solubility of PVME into micelle core is very limited for all of the blends.

Above LCST, a micellar phase (M) was separated into two phases (M1 + L2) of different PVME fractions by the decrease of specific interaction between styrene block and PVME. As the content of PVME decreased on heating, the interdomain distance of the blend was reduced and was very close to that of pure block copolymer above 230 °C. On further heating, the mesophase M1 for all fractions underwent an order–disorder transition at almost the same temperature as pure block copolymer. This indicates that the SI72/PVME blend is almost completely macrophase-separated above 230 °C.

Acknowledgment. This work was supported by the Korea Research Foundation (KRF-96-011-E0034). The SAXS measurements were performed at the Pohang Accelerator Laboratory (Beamline 1B2 and 3C2). The authors thank Prof. K. Cho and Mr. H. Yang at POSTECH for help with cryo-TEM experiments.

References and Notes

- (1) Bates, F. S.; Schulz, M. F.; Khandpur, A. K.; Förster, S.; Rosedale, J. H.; Almdal, K.; Mortensen, K. *Faraday Discuss.* **1994**, *98*, 7.
- (2) Ahn, J.-H.; Zin, W.-C. *Macromolecules* **2000**, *33*, 641.

- (3) Zin, W.-C.; Roe, R.-J. *Macromolecules* **1984**, *17*, 183.
- (4) Roe, R.-J.; Zin, W.-C. *Macromolecules* **1984**, *17*, 189.
- (5) Tanaka, H.; Hasegawa, H.; Hashimoto, T. *Macromolecules* **1991**, *24*, 240.
- (6) Whitmore, M. D.; Noolandi, J. *Macromolecules* **1985**, *18*, 2486.
- (7) Winey, K. I.; Thomas, E. L.; Fetters, L. J. *Macromolecules* **1992**, *25*, 422.
- (8) Selb, J.; Marie, P.; Rameau, A.; Duplessix, R.; Gallot, Y. *Polym. Bull.* **1983**, *10*, 444.
- (9) Rigby, D.; Roe, R.-J. *Macromolecules* **1984**, *17*, 1778.
- (10) Rigby, D.; Roe, R.-J. *Macromolecules* **1986**, *19*, 721.
- (11) Roe, R.-J. *Macromolecules* **1986**, *19*, 728.
- (12) Nojima, S.; Roe, R.-J.; Rigby, D.; Han, C. C. *Macromolecules* **1990**, *23*, 4305.
- (13) Kinning, D. J.; Thomas, E. L.; Fetters, L. J. *J. Chem. Phys.* **1989**, *90*, 5806.
- (14) Kinning, D. J.; Winey, K. I.; Thomas, E. L. *Macromolecules* **1988**, *21*, 3502.
- (15) Kinning, D. J.; Thomas, E. L. *Macromolecules* **1984**, *17*, 1712.
- (16) Tucker, P. S.; Barlow, J. W.; Paul, D. R. *Macromolecules* **1988**, *21*, 1678.
- (17) Tucker, P. S.; Barlow, J. W.; Paul, D. R. *Macromolecules* **1988**, *21*, 2794.
- (18) Hashimoto, T.; Kimishima, K.; Hasegawa, H. *Macromolecules* **1991**, *24*, 5704.
- (19) Kimishima, K.; Hashimoto, T.; Han, C. D. *Macromolecules* **1995**, *28*, 3842.
- (20) Lee, H.-K.; Kang, C.-K.; Zin, W.-C. *Polymer* **1996**, *37*, 287.
- (21) Lee, H.-K.; Kang, C.-K.; Zin, W.-C. *Polymer* **1997**, *38*, 1595.
- (22) Izuka, N.; Bodycomb, J.; Hasegawa, H.; Hashimoto, T. *Macromolecules* **1998**, *31*, 7256.
- (23) Ahn, J.-H.; Kang, C.-K.; Zin, W.-C. *Eur. Polym. J.* **1997**, *33*, 1113.
- (24) Hashimoto, T.; Izumitani, T.; Oono, K. *Macromol. Symp.* **1995**, *98*, 925.
- (25) Kim, J. K.; Lee, H. H.; Son, H. W.; Han, C. D. *Macromolecules* **1998**, *31*, 8566.
- (26) Shimoi, T.; Hamada, F.; Nasako, T.; Yoneda, K.; Imai, K.; Nakajima, A. *Macromolecules* **1990**, *23*, 229.
- (27) Percus, J. K.; Yevick, G. J. *Phys. Rev.* **1958**, *110*, 1.
- (28) Ashcroft, N. W.; Lekner, J. *Phys. Rev.* **1966**, *145*, 83.
- (29) Kotlarchyk, M.; Chen, S.-H. *J. Chem. Phys.* **1983**, *79*, 2461.
- (30) Kim, J. R.; Jamieson, A. M.; Hudson, S. D.; Manas-Zloczower, I.; Ishida, H. *Macromolecules* **1998**, *31*, 5383.
- (31) Koizumi, S.; Hasegawa, H.; Hashimoto, T. *Macromolecules* **1994**, *27*, 6532.
- (32) Koizumi, S.; Hasegawa, H.; Hashimoto, T. *Makromol. Chem., Macromol. Symp.* **1992**, *62*, 75.

MA001642+